

# NODE-SPECIFIC EFFECTS IN LATENT SPACE MODELLING OF MULTIDIMENSIONAL NETWORKS

Silvia D'Angelo, Marco Alfò, Thomas Brendan Murphy

August 1, 2022

## Abstract

Observed multidimensional network data can have different levels of complexity, as nodes may be characterized by heterogeneous individual-specific features. Also, such characteristics may vary across the networks. This article discusses a novel class of models for multidimensional networks, able to deal with different levels of heterogeneity within and between networks. The proposed framework is developed within the family of latent space models, in order to distinguish recurrent symmetrical relations between the nodes from node-specific features in the different views. Models parameters are estimated via a Markov Chain Monte Carlo algorithm. Simulated data and also FAO fruits import/export data are analysed to illustrate the performances of the proposed models.

**Keywords:** Latent Space Models, Multiplex, Markov Chain Monte Carlo

## 1 Introduction

Relational data can be, and often are, represented in the form of networks. Within a network, dyadic relations are coded as edges binding units, the nodes, among which the relations are recorded. When multiple relations are recorded among the same group of nodes, a multidimensional network (multiplex) is observed. Instead, if the same relation is observed through time on the same set of units, a dynamic network can be defined. Observed network data, either uni-dimensional or multidimensional, can exhibit different characteristics, that directly influence their structure. A quite studied one is *transitivity*, which refers to whether the relation being represented in the network is, up to some extent, transitive. In simpler words, transitivity is described by the “a friend of my friend is my friend” phenomenon in social networks. A popular way to model such feature is through latent space models, first introduced by Hoff et al. (2002). The basic idea is to represent the nodes in a low-dimensional, unobserved space, and postulate that the probabilities of observing edges in the network depend on the positions of the nodes in such space. Different latent space approaches have been proposed in the literature, based on metrics Hoff et al. (2002), Hoff (2005), or ultrametrics Schweinberger and Snijders (2003). Among metric latent spaces, models based on Euclidean distance are probably the most widespread, as they produce easily interpretable representations of the networks while being flexible enough to describe a large variety of network data. Alternatives to the distance latent space model are the projection model by Hoff et al. (2002) and the multiplicative latent space model by Hoff (2005); both postulating that the edge probabilities

depend on the inner products of the latent coordinates. Such models address transitivity differently from distance model, as they incorporate in the latent space representation of the nodes also the “direction” of the relations [Hoff et al. \(2002\)](#). Extensions of the latent space models to multidimensional networks are those of [Gollini and Murphy \(2016\)](#), [Salter-Townshend and McCormick \(2017\)](#), [Hoff \(2011\)](#) and [D’Angelo et al. \(2018\)](#). [Sewell and Chen \(2015\)](#) introduced a latent space model for binary dynamic networks, and later has extended it to include weighted dynamic networks [Sewell and Chen \(2016\)](#). [Durante and Dunson \(2016\)](#) developed a framework based on a dynamic latent space to model dynamic networks of face-to-face contacts among individuals.

Another interesting feature is that of *degree heterogeneity*, which refers to the propensity of some nodes to send/receive more edges than others. [Holland and Leinhardt \(1981\)](#) proposed the so called “ $p_1$ ” model, where nodes sender and receiver effects are treated as random effects. [van Duijn et al. \(2004\)](#) developed the “ $p_2$ ” model, an extension of the “ $p_1$ ” model, where node-specific attributes are introduced in the form of covariates, together with the sender/receiver random effects. Other extensions of such model are that by [Hoff \(2003\)](#) and [Hoff \(2005\)](#), that bring together sender/receiver effects and latent space models for single networks. Part of the framework was later extended by [Krivitsky et al. \(2009\)](#), to allow for clustering of the nodes in the latent space. In the context of dynamic networks, [Sewell and Chen \(2015\)](#) model the overall sender/receiver effect in the networks, investigating whether activity (sending links) or popularity (receiving links) is more important in the edge formation process.

Using latent space models as a starting point, we develop an Euclidean latent space distance framework to model transitivity and heterogeneity in multidimensional networks. Our aim is to extend the model by [D’Angelo et al. \(2018\)](#) to account for degree heterogeneity and to model different levels of complexity in multidimensional networks. Indeed, multidimensional networks data are complex in two directions: in the number of nodes and in the number of views. A model that aims at describing the interactions between the actors in such an high dimensional complex should aim both at explaining the view-specific features, but also at being parsimonious with respect to the number of parameters to be considered. Therefore, we propose to model transitivity via single latent space, common for the whole multiplex; the distances in such space represent the overall associations between the nodes. Then, heterogeneity across different networks will be addressed via the introduction of node-specific sender/receiver parameters, that will account both for intra(-) and inter(-) networks degree heterogeneity.

The paper is organized as follows: section 2 introduces more formally to the concept of multidimensional networks and defines the proposed class of models for direct multiplexes. Section 3 provides with the details of the estimation procedure implemented and discusses some issues linked to model identifiability and how to address them. Section 4 extends the class of models proposed in section 2 to the particular case of undirected multidimensional network data. A simulation study is conducted in Section 5, to investigate the properties of the novel class of models, and an heuristic procedure for model selection is presented. Then, an application on FAO trade data is presented in Section 6. Last, we conclude with a discussion in Section 7.

## 2 Models

The data we model are binary multidimensional networks, referred to also as multiplexes. A multiplex  $\mathbf{Y}$  is a complex object defined by a collection of networks (views). These networks can be represented by  $n \times n$  adjacency matrices  $\{y^{(1)}, \dots, y^{(K)}\} = \mathbf{Y}$ , where the index  $k = 1, \dots, K$  indicates the different views. The entries of each matrix can take two values,  $y_{ij}^{(k)} = 1$  when nodes  $(i, j)$  in the  $k^{\text{th}}$  network are joined by an edge, and  $y_{ij}^{(k)} = 0$ , when they are not. Views in a multiplex share the same set of nodes, whose cardinality is denoted by  $n$ . In the present context, nodes will be indexed by  $i, j = 1, \dots, n$ . A multiplex can be either undirected, if  $y_{ij}^{(k)} = y_{ji}^{(k)}$  or directed, if the adjacency matrices are not symmetrical,  $y_{ij}^{(k)} \neq y_{ji}^{(k)}$ . In general, real world multiplexes are hardly undirected, but different levels of ‘‘symmetry’’ can be observed in the adjacency matrices. Notice that, even if a network is undirected, this does not imply that all the nodes have the same number of connections, that is, the same degree. Modelling the degree, or, for directed networks, the out-degree,  $\sum_{j \neq i} y_{ij}^{(k)}$ , and the in-degree,  $\sum_{j \neq i} y_{ji}^{(k)}$ , is a task that might be of interest in many empirical applications. Indeed, it can help recover the most influential, or popular, nodes in a network, or the more active ones. Also, different networks might exhibit different levels of heterogeneity in the nodes degree distribution. In that sense, multidimensional networks are heterogeneous in two directions: within and between the views. In this work, we introduce a class of latent space model that address transitivity and this double font of heterogeneity in the analysis of multiplexes. In this section, we will introduce the more general latent space framework for directed multidimensional networks.

With latent space models based on Euclidean distances, we assume that each node is located into an unobserved  $p$ -dimensional Euclidean space; the probability of having an edge between the dyad  $(i, j)$ , conditionally on the latent coordinates  $z_i$ ,  $i = 1, \dots, n$ , of the nodes, is independent on all the other nodes positions [Hoff et al. \(2002\)](#). We will maintain the assumptions in our model, together with an additional one. Indeed, we assume the probability of a connection between nodes  $i$  and  $j$  also depends on their individual propensities to send/receive links. In multidimensional networks, the propensities may vary with the views, as an actor could be quite popular in a network, but do not receive edges in another one of the collection. Different levels of heterogeneity in edge probabilities will then depend on different levels of heterogeneity in the behaviour of the nodes in the different networks.

Let us define two parameters:  $\theta_i^{(k)}$  and  $\gamma_i^{(k)}$ ,  $i = 1, \dots, n$  and  $k = 1, \dots, K$ . The first one is the sender parameter for node  $i$  in the  $k^{\text{th}}$  network. The second is the receiver parameter for node  $i$  in the  $k^{\text{th}}$  network. They are assumed to be proportional to, respectively, the propensity of a given node  $i$  to send/receive edges.

			$\gamma_j^{(k)}$	
	0	$\gamma_j$	$\gamma_j^{(k)}$	
	0	NN	NC	NV
$\theta_i^{(k)}$	$\theta_i$	CN	CC	CV
	$\theta_i^{(k)}$	VN	VC	VV

Table 1: The class of models defined by the inclusion of sender and receiver effects and their different specifications.

Then, the probability  $p_{ij}^{(k)}$  of a connection from node  $i$  to node  $j$ , in the  $k^{\text{th}}$  network, depends on the couple of parameters  $(\theta_i^{(k)}, \gamma_j^{(k)})$ . More specifically, we take it to be defined by:

$$p_{ij}^{(k)} = P\left(y_{ij}^{(k)} = 1 \mid \Omega^{(k)}, \theta_i^{(k)}, \gamma_j^{(k)}, d_{ij}\right) = \frac{\exp\{f(\alpha^{(k)}, \theta_i^{(k)}, \gamma_j^{(k)}) - \beta^{(k)} d_{ij}\}}{1 + \exp\{f(\alpha^{(k)}, \theta_i^{(k)}, \gamma_j^{(k)}) - \beta^{(k)} d_{ij}\}} \quad (1)$$

Where  $\Omega = (\Omega^{(1)}, \dots, \Omega^{(K)}) = (\alpha^{(1)}, \dots, \alpha^{(K)}, \beta^{(1)}, \dots, \beta^{(K)})$  is the set of network-specific parameters, and  $d_{ij}$  is the squared Euclidean distance between node  $i$  and node  $j$  in the  $p$ -dimensional latent space.

According to the various behaviours of the nodes, we can define three different “status” for each type of parameter:

- *absent*:  $\theta_i^{(k)} = 0$  or  $\gamma_j^{(k)} = 0$ , for  $i = 1, \dots, n$  and  $k = 1, \dots, K$ ;
- *present and constant*:  $\theta_i^{(k)} = \theta_i$ ,  $\gamma_j^{(k)} = \gamma_j$ , for  $i = 1, \dots, n$  and  $k = 1, \dots, K$ ;
- *present and variable*:  $\theta_i^{(k)}$  or  $\gamma_j^{(k)}$ , for  $i = 1, \dots, n$  and  $k = 1, \dots, K$ .

Note that we assume the same type of effect (absent, constant and variable) for all the networks. Hence, if for example  $\mathbf{Y}^{(k)}$  has a constant receiver effect, then all the other  $K - 1$  networks have constant receiver effect too. A relaxation of this assumption is presented in the section 7. Table 1 presents a schematic taxonomy of the 9 potentially different models arising from this definition of the sender and receiver effects.

The effect of the sender/receiver parameters on the edge probabilities can be made explicit defining the collection of network-specific matrices  $\Phi = (\Phi^{(1)}, \dots, \Phi^{(K)})$ , with elements

$$\left[\phi_{ij}^{(k)}\right] = \left[\frac{\theta_i^{(k)} + \gamma_j^{(k)}}{g}\right], \quad (2)$$

and the auxiliary variable  $g$  as:

$$g = \begin{cases} 0 & \text{if both sender and receiver effects are absent,} \\ 1 & \text{if only one between sender and receiver effects is present,} \\ 2 & \text{if both sender and receiver effects are present.} \end{cases} \quad (3)$$

Then, we can define the function  $f(\cdot)$  as:

$$f(\alpha^{(k)}, \theta_i^{(k)}, \gamma_j^{(k)}) = f(\alpha^{(k)} \phi_{ij}^{(k)}) = (1 - \mathbf{I}_{(0)}(g)) \alpha^{(k)} \phi_{ij}^{(k)} + \mathbf{I}_{(0)}(g) \alpha^{(k)}. \quad (4)$$

with

$$\mathbf{I}_{(0)}(g) = \begin{cases} 1 & \text{if } g = 0 \\ 0 & \text{if } g \neq 0 \end{cases}.$$

Equations 1, 2 and 4 explicit a modelling assumption, that is: inside each view, sender and receiver parameters jointly impact on the intercept. Differently from an additive sender and receiver effect specification (Krivitsky et al. (2009)), and as in latent space models without such type of effects, this assumption implies that the intercepts  $\alpha^{(k)}$  still correspond, on the logit scale, to the maximum value achievable for edge probabilities in the networks. Furthermore, if we assume that

$$\gamma_j^{(k)}, \theta_i^{(k)} \sim Unif(-1, 1), \quad i, j = 1, \dots, n$$

and recall the definition of  $\phi_{ij}^{(k)}$  (2) and of  $g$  (3), we notice that we are able to treat sender and receiver effects as relative effects. Indeed, inactive (or unpopular) nodes will have a value of the effect close to  $-1$ , while active (or popular) nodes will have a value of the parameter close to  $1$ . Notice that their combined effect  $\phi_{ij}^{(k)}$  also varies in the same range. Bounding these parameters in the interval  $[-1, 1]$  allows to easily interpret the differences in levels of activity (or popularity) of the nodes. However, allowing the  $\phi_{ij}^{(k)}$  to be negative, implies that if  $\alpha^{(k)} < 0$  and  $\phi_{ij}^{(k)} < \phi_{il}^{(k)} < 0$ , then  $p_{ij}^{(k)} > p_{il}^{(k)}$  and this would violate the assumption that sender and receiver effects are directly proportional to edge probabilities. To avoid such an issue, we bound the intercept to be non-negative,  $\alpha^{(k)} \geq 0 = LB(\alpha)$ ,  $k = 1, \dots, K$ . This imposition does not alter the interpretation of the intercepts and other model parameters. Also, fixing a lower bound for the intercepts does not imply a lower bound for the edge probabilities, as the impact of the latent space might decrease the effect of the intercept and the sender/receiver parameters.

Note also, from equation 4, that when no sender or receiver effect is present, the edge probabilities in equation 1 reduce to that of the model presented in D’Angelo et al. (2018) (model  $NN$  in table 1). As for this model, inference procedures have already been provided, from the next section we will focus on the eight models that include at least one type of effect. For these models, the edge probability formula presented in equation 1 can be rewritten as:

$$p_{ij}^{(k)} = \frac{\exp\{\alpha^{(k)}\phi_{ij}^{(k)} - \beta^{(k)}d_{ij}\}}{1 + \exp\{\alpha^{(k)}\phi_{ij}^{(k)} - \beta^{(k)}d_{ij}\}} \quad (5)$$

### 3 Estimation

We propose a hierarchical Bayesian approach to estimate the class of latent space models proposed in section 2. The corresponding (log-)likelihood can be derived from equation (5),

$$\ell(\Omega, \Phi, D | \mathbf{Y}) = \sum_{k=1}^K \sum_{\substack{i=1 \\ j \neq i}} \ell_{ij}^{(k)} = \sum_{k=1}^K \sum_{\substack{i=1 \\ j \neq i}} y_{ij}^{(k)} \log(p_{ij}^{(k)}) + (1 - y_{ij}^{(k)}) \log(1 - p_{ij}^{(k)}). \quad (6)$$

The prior distributions for the model parameters are:

$$\begin{aligned} \beta^{(k)} &\sim N_{(0, \infty)}(\mu_\beta, \sigma_\beta^2), & \alpha^{(k)} &\sim N_{(0, \infty)}(\mu_\alpha, \sigma_\alpha^2), \\ z_i &\sim MVN_p(\mathbf{0}, I), & \gamma_j^{(k)}, \theta_i^{(k)} &\sim Unif(-1, 1), \end{aligned}$$

where  $\mu_\beta, \mu_\alpha, \sigma_\beta^2, \sigma_\alpha^2$  are nuisance parameters whose specification could be relevant. Hence, to avoid subjectivity, we introduce an extra layer of dependence and model them with the following (hyper) prior distributions:

$$\mu_r | \sigma_r^2 \sim N_{(0, \infty)}(m_r, \tau_r \sigma_r^2), \quad \sigma_r^2 \sim \text{Inv}\chi_{\nu_r}^2,$$

for  $r = \alpha, \beta$ . The hyperparameters  $m_\alpha, m_\beta, \tau_\alpha, \tau_\beta, \nu_\alpha, \nu_\beta$  have to be specified by the users. Figure 1 provides a representation of the hierarchical structure of the proposed models.

#### 3.1 Identifiability

Note that, for identifiability reasons, network intercept and coefficient must be fixed in one of the  $K$  networks, which we will refer to as the “reference” network. Fixing these two parameters is not enough, as the multiplicative

effect of  $\phi_{ij}^{(k)}$  can still cause problems. To avoid such issues, one sender and one receiver effect should be fixed in each view, if both are present. When the effect is variable, we propose to choose, in each network, the node  $i$  with the highest observed out-degree (or in-degree) and fix  $\theta_i^{(k)} = 1$  (or  $\gamma_i^{(k)} = 1$ ). Instead, with a constant effect, we propose to select the node  $i$  with the highest observed mean out-degree (or mean in-degree) and fix  $\theta_i = 1$  (or  $\gamma_i = 1$ ). Fixing the sender and/or receiver parameter for one node does not change the interpretation of the model. Indeed, we are most interested in ordering the nodes with respect to the sender and/or receiver effects and rather than in the actual numeric values of these parameters.

### 3.2 MCMC algorithm

We propose an MCMC algorithm to estimate model parameters proposed in 2. Our algorithm iterates over the model parameters, the latent coordinates and the nuisance parameters; full conditionals in closed form are available only for the nuisance parameters. To update the other quantities we use a Metropolis-Hastings step. The full conditional distributions for the nuisance parameters, the proposal distributions for the network-specific parameters and the latent coordinates are presented in appendix B, together with the proposal distributions for sender/receiver parameters. The procedure first simulate a new value for each nuisance parameter. Then, it proposes a new value for the network intercept and the network coefficient, with a joint MH step on each network. Later, another MH step sequentially proposes new latent coordinates values. As the likelihood in equation (6) is invariant to rotations and translations of the latent coordinates, when a new set of positions is defined, Procrustes correlation is employed to check whether this new set is just a simple transformation of the set at the precedent iteration. If so, the new set is discarded in favour of the previous one. After that, sender/receiver parameters are updated sequentially on the nodes, but jointly over the different networks via an MH step. The joint update is performed to speed up the calculations, given the high number of model parameters. When both effects are updated, a new collection of  $\Phi^{(k)}$  is computed.

The latent coordinates are initialized via multidimensional scaling on the average geodesic distances over the different networks. Squared Euclidean distances are then computed on the starting latent positions. The distances are used to perform a logistic regression of the adjacency matrices and the intercept and coefficient estimates are used to initialize  $\alpha^{(k)}$  and  $\beta^{(k)}$ . The sender and receiver parameters are initialized in a non-informative way, fixing them all to 0.

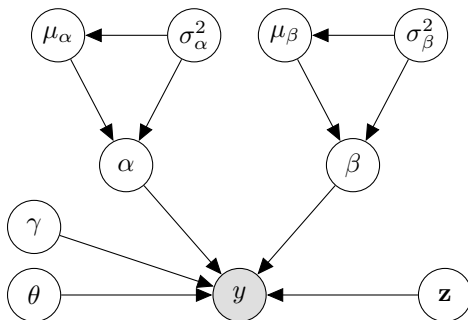


Figure 1: Hierarchy structure of the model.

Edge specific covariates, either constant or variable with the networks can be easily incorporated in the framework, when defining the edge probabilities. Also, the model can be easily extended to deal with the presence of missing edges in the data or missing nodes. The full conditional and proposal distributions for the model parameters presented in Appendix B are derived for the most general case of missing data and edge-specific covariates.

## 4 Undirected network

In the particular case of undirected networks, out-degrees and in-degrees are identical for each node. The framework proposed in section 2 can be easily adjusted to the context of undirected multidimensional networks. In such a contest we will have to impose the constrain:  $\theta_i^{(k)} = \gamma_i^{(k)} = \delta_i^{(k)}$ , for all  $i = 1, \dots, n$ . Then, the edge probability equation (5) can be rewritten as:

$$P\left(y_{ij}^{(k)} = 1 \mid \Omega^{(k)}, \delta_i^{(k)}, \delta_j^{(k)}, d_{ij}\right) = \frac{\exp\left\{\alpha^{(k)} \frac{\delta_i^{(k)} + \delta_j^{(k)}}{2} - \beta^{(k)} d_{ij}\right\}}{1 + \exp\left\{\alpha^{(k)} \frac{\delta_i^{(k)} + \delta_j^{(k)}}{2} - \beta^{(k)} d_{ij}\right\}} \quad (7)$$

This effect, if present, can either be variable across the different networks,  $\delta_i^{(k)}$ , or constant,  $\delta_i^{(k)} = \delta_i$ , for each  $k = 1, \dots, K$  and  $i = 1, \dots, n$ . Appendix B provides the reader with the proposal distribution formulated to estimate these parameter.

## 5 Simulations

We constructed a simulation study to evaluate the properties of the proposed estimation procedure for the novel class of models, where we examine the consistence of the estimates of the model parameters. Multidimensional networks are simulated from the models *NC*, *NV*, *CC*, *CV* and *VV*. Then, we fit, for each one of the simulated multiplexes, the “true” model, that is, the model a given multiplex was simulated from. These five models are chosen to investigate the consistency properties of the estimators with different numbers of parameters in the models. A first block of simulated multidimensional networks, **B1**, has dimensions ( $n = 50, K = 5$ ). A second, larger, one, **B2**, has dimensions similar to those of the multiplex used in the application in section 6, namely ( $n = 50, K = 10$ ).

In both the simulation scenarios, we set  $\alpha^{(1)} = 2$  and  $\beta^{(1)} = 1$ . The prior parameters are  $\nu_\alpha = \nu_\beta = 3$ ,  $m_\alpha = 2$ ,  $m_\beta = 0$ ,  $\tau_\alpha = \tau_\beta = (K - 1)/K$  and  $p = 2$ . Small variations of these values have been tried and did not affect the simulation results. Also, there are no missing edges in the simulated data. The MCMC algorithm run for 60000 iterations with a burn in of 15000.

Table 3 shows the average values of the distance correlation computed between the simulated and estimated edge probabilities, for all the different networks composing the multiplexes in blocks **B1** and **B2**. These correlations are always high, proving that we can well reconstruct the edge probability distributions, regardless of the specified model, a given view or of the dimensions of the multiplex. Also, last column of Table 3 reports the average values of the Procrustes correlation between the simulated and the estimated latent spaces. As for the edge probabilities, we see that the latent coordinates are appropriately recovered. To evaluate the estimates of the sender/receiver parameters in the different models, we compute, for each network, the Spearman correlation

coefficient between the simulated and the estimated parameters. This coefficient is employed as we are mainly interested in recovering the ordering of the nodes, with respect to the two effects. Indeed, sender and receiver parameters vary in a relatively small interval,  $(-1, 1)$ , and the exact numerical values might not be of much interest. Table 4 reports, for each network of each multiplex, the average values of the Spearman correlation coefficient between the  $n$ ,  $n = 50$ , simulated and estimated receiver parameters,  $\gamma_i^{(k)}$ . These values are always much greater than 0.5, with a couple of exceptions for some networks in the models with higher complexity, that is  $CV$  and  $VV$ . However, as we could see from Table 3, this did not impact the reconstruction of the edge probabilities. Table 2 reports the average values of the Spearman correlation coefficient between the  $n$ ,  $n = 50$ , simulated and estimated sender parameters,  $\theta_i^{(k)}$ . The behaviour of these estimates complies with those of the receiver parameters (Table 4), proving that the two effects, when both presents, are estimated equally good.

We refer to Appendix C for the results on the estimates of intercept,  $\alpha^{(k)}$ , and scale coefficient parameters,  $\beta^{(k)}$ . The intercepts are recovered within a 95% credible interval, with two small exceptions which occur when the simulated values are “extreme”. However, the ordering between the different intercepts in a given multiplexes is always recovered. Instead, the scale coefficients tend to be overestimated. However, also in this case, the ordering between different coefficients in a multiplex is recuperated. The overestimation of the scaling coefficients is caused by an underestimation of the latent distances. Indeed, the simulated and estimated products between distances and scale coefficients are well recovered. Precise point estimates of all the parameters are quite hard to recover, due to the large number of parameters of these models. However, the aim of these class of latent space models is to describe different features of a multiplex by means of comparisons between different nodes and networks. This intent is met, as we are always able to recover the ordering between the nodes and the views.

		$k = 1$	$k = 2$	$k = 3$	$k = 4$	$k = 5$	$k = 6$	$k = 7$	$k = 8$	$k = 9$	$k = 10$
B1	CC	0.84	0.84	0.84	0.84	0.84	-	-	-	-	-
	CV	0.90	0.90	0.90	0.90	0.90	-	-	-	-	-
	VV	0.58	0.57	0.55	0.58	0.59	-	-	-	-	-
B2	CC	0.78	0.78	0.78	0.78	0.78	0.78	0.78	0.78	0.78	0.78
	CV	0.79	0.79	0.79	0.79	0.79	0.79	0.79	0.79	0.79	0.79
	VV	0.65	0.66	0.66	0.65	0.66	0.66	0.66	0.66	0.67	0.65

Table 2: For the models in the first block of simulations with sender effect, it is reported the value of the Spearman correlation index between the simulated and the estimated sender effects, for the different networks in the multiplexes.



		$k = 1$	$k = 2$	$k = 3$	$k = 4$	$k = 5$	$k = 6$	$k = 7$	$k = 8$	$k = 9$	$k = 10$	PC
B1	NC	0.86	0.84	0.86	0.87	0.85	-	-	-	-	-	0.94
	NV	0.87	0.87	0.87	0.85	0.86	-	-	-	-	-	0.92
	CC	0.89	0.89	0.90	0.91	0.87	-	-	-	-	-	0.96
	CV	0.84	0.81	0.83	0.84	0.85	-	-	-	-	-	0.90
	VV	0.83	0.81	0.80	0.81	0.81	-	-	-	-	-	0.93
B2	NC	0.89	0.84	0.83	0.83	0.81	0.92	0.84	0.81	0.81	0.82	0.85
	NV	0.83	0.80	0.79	0.76	0.81	0.78	0.88	0.71	0.75	0.75	0.93
	CC	0.83	0.87	0.91	0.84	0.90	0.91	0.91	0.84	0.86	0.91	0.90
	CV	0.75	0.86	0.87	0.76	0.86	0.88	0.87	0.86	0.83	0.87	0.91
	VV	0.73	0.72	0.82	0.85	0.88	0.79	0.79	0.79	0.86	0.84	0.90

Table 3: For each one of the models in the first block of simulations, it is reported the distance correlation between the simulated and the estimated edge-probabilities, for the different networks in the multiplexes. Last column PC shows the value of the Procrustes correlation between the simulated and the estimated latent space. “B1” stands for the multiplexes with  $n = 50$  and  $K = 5$  and “B2” for the multiplexes with  $n = 50$  and  $K = 10$ .

		$k = 1$	$k = 2$	$k = 3$	$k = 4$	$k = 5$	$k = 6$	$k = 7$	$k = 8$	$k = 9$	$k = 10$
B1	NC	0.84	0.84	0.84	0.84	0.84	-	-	-	-	-
	NV	0.85	0.80	0.86	0.92	0.91	-	-	-	-	-
	CC	0.84	0.84	0.84	0.84	0.84	-	-	-	-	-
	CV	0.80	0.86	0.81	0.73	0.6	-	-	-	-	-
	VV	0.67	0.61	0.50	0.64	0.75	-	-	-	-	-
B2	NC	0.94	0.94	0.94	0.94	0.94	0.94	0.94	0.94	0.94	0.94
	NV	0.92	0.86	0.84	0.74	0.84	0.83	0.92	0.61	0.80	0.79
	CC	0.84	0.84	0.84	0.84	0.84	0.84	0.84	0.84	0.84	0.84
	CV	0.51	0.66	0.83	0.50	0.73	0.82	0.82	0.85	0.61	0.79
	VV	0.61	0.48	0.81	0.83	0.86	0.58	0.54	0.57	0.87	0.59

Table 4: For each one of the models in the first block of simulations, it is reported the value of the Spearman correlation index between the simulated and the estimated receiver effects, for the different networks in the multiplexes.

## 5.1 Heuristic procedure for model selection

In Section 2 we have proposed 9 models for multidimensional networks. Hence, we provided 9 different alternatives to model any multiplex. In general, the issue of model selection can be addressed in two different ways. A first approach is that of an expert, that has some previous knowledge on the data and believes a particular model should be used. A second, more common, approach, is that of computing some model selection criteria.

Note that, in the present context, the estimation of all the nine models, given an observed multiplex, may request some (computational) time, especially when the number of nodes is large.

Hence, we propose to decide which model to estimate a priori. In particular, we propose to determine the model to fit on the basis of the correlations between the observed in-degrees and out-degrees of the networks in a multiplex. The general idea is that computing the correlations among networks out-degree/in-degree distributions could serve as a proxy of the heterogeneity within and between the views. Let us define  $\mathbf{S} = [s_{ik}]$  the matrix of the observed out-degrees and  $\mathbf{R} = [r_{ik}]$  the matrix of the observed in-degrees. Both matrices have dimension  $n \times K$ , where  $n$  is the number of nodes and  $K$  the number of networks. Then, the matrices  $cor(S) = c_{s_k}$  and  $cor(R) = c_{r_k}$  contain the values of the correlation of the sender/receiver effects between views. Instead, the matrices  $cor(S^T) = c_{s_i}$  and  $cor(R^T) = c_{r_i}$  include the correlations of the sender/receiver effects between nodes. Let us now define  $\bar{c}_{s_k}$ ,  $\bar{c}_{r_k}$ ,  $\bar{c}_{s_i}$  and  $\bar{c}_{r_i}$  the mean values among all the cells of the matrices introduced above and  $sd(c_{s_k})$ ,  $sd(c_{r_k})$ ,  $sd(c_{s_i})$  and  $sd(c_{r_i})$  the corresponding standard deviations. We propose to use such quantities to choose which type of model has to be estimated, given an observed multidimensional network. We have defined an heuristic procedure that is able to operate the task, and it is described in the scheme in Figure 2. Observed multiplexes with similar values of  $\bar{c}_{s_k}$  and  $\bar{c}_{r_k}$ , and of  $\bar{c}_{s_i}$  and  $\bar{c}_{r_i}$ , could have similar types of sender and receiver effects. On the contrary, a multiplex that exhibit conflicting values of sender and receiver correlation among views or among nodes might come from a model where the two effects are of different types. In this latter case, the higher the discrepancy between sender and receiver “node” correlations, the higher the chance that the underlying model has two most different types of effect, that is, one null and one variable. Whether the most complex effect is the sender or the receiver one is decided by looking at  $\bar{c}_{r_k}$  and  $\bar{c}_{s_k}$ . The smallest of the two determines which effect should be the less complex. When the sender/receiver effects are selected to be of the same type, a low correlation among views and the presence of variability between the nodal correlations indicate that the underlying model is the most complex one, the *VV* model. Instead, the choice between the *NN* and the *CC* model is operated looking at the values  $\bar{c}_{s_i}$  and  $\bar{c}_{r_i}$ . If these values are high, that is, if they exceed the threshold  $c_2$ , the procedure proposes a *NN* model. Otherwise it chooses the *CC* model.

As it can be seen from the scheme in Figure 2, this procedure depends on four thresholds:  $\epsilon_1$ ,  $\epsilon_2$ ,  $c_1$  and  $c_2$ . We tested the performance of the proposed procedure via simulations and the results are presented in Appendix D. In the simulation setting, we have run the procedure on two groups of 10000 multidimensional networks. The first multiplex has dimensions  $(50 \times 10)$ , while the second one has dimensions matching with those of the multiplex studied in the application in Section 6,  $(65 \times 10)$ . The thresholds have been fixed via cross validation and are  $\epsilon_1 = 0.12$ ,  $\epsilon_2 = 0.2$ ,  $c_1 = 0.5$ ,  $c_2 = 0.8$ . The procedure proved to be fast and to give reliable results. Indeed, on average, the “true” model is chosen 90% of the times. Also, when the heuristic procedure fails to select the right model, it proposes a model that is quite similar to the “true” one. For example, when a multiplex of dimension  $(65 \times 10)$  is simulated from a *VV* model, the procedure returns the *VV* model 90% of the times

and the other 10% it chooses the *CC* model.

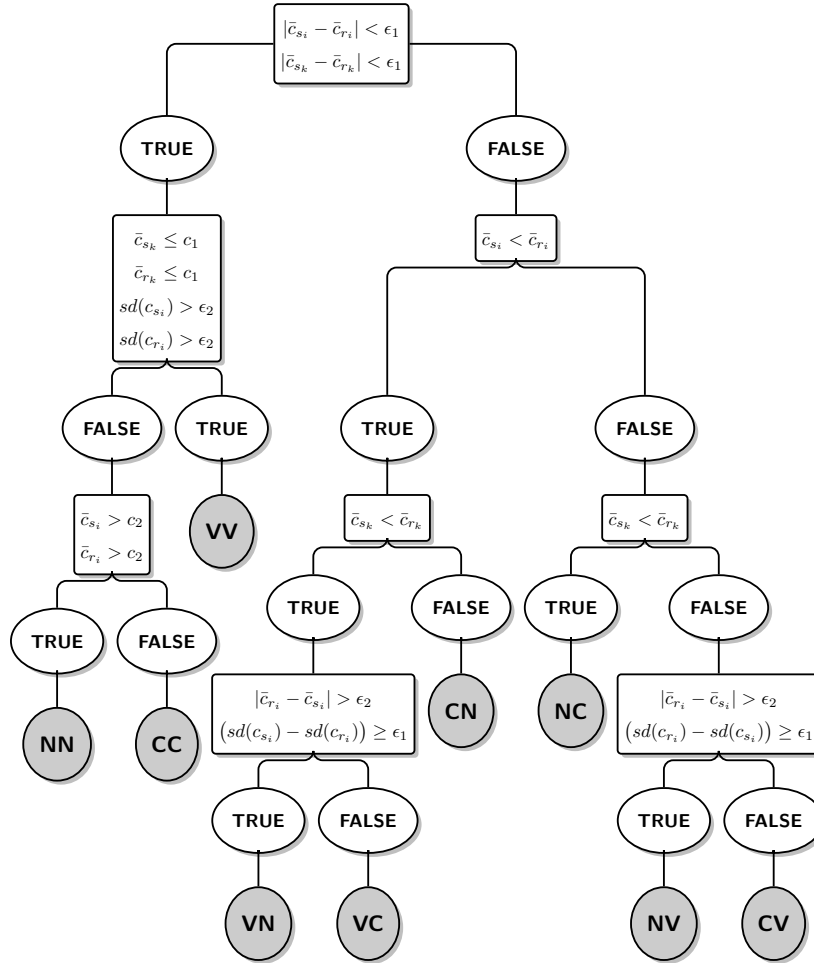


Figure 2: Schematic representation of the heuristic procedure implemented to select the model to be estimated. The thresholds have been fixed via cross validation and are:  $\epsilon_1 = 0.12$ ,  $\epsilon_2 = 0.2$ ,  $c_1 = 0.5$ ,  $c_2 = 0.8$ .

## 6 FAO trade data

FAO food and agricultural trade data, measuring annual import/exports between countries, are analysed. The data are available at FAO website (FAOStat, 2013) and the most recent subset refers to the year 2013. Here we consider the fruit sub-market. In particular, we focus on fresh fruit, as fresh items are the most traded internationally. For illustrative reasons, we consider a restricted number of fruits, and we choose 10 amongst the most commonly consumed and traded: “Grapes”, “Watermelons”, “Apples”, “Oranges”, “Pears”, “Bananas”, “Pineapples”, “Tangerines, mandarins, clementines, satsuma”, “Plantains” and “Grapefruit (inc. pomelos)”. The original data register the volume of the trade, that is, the quantity traded among couples of countries. We focus on the presence/absence of an import/export relation between couples of countries. Our aim is to verify whether close countries are more likely to trade, comparing the estimated latent coordinates of the countries with the geographical ones. Also, we can address which countries are more relevant in the exchange of fruits, via the estimated sender and receiver parameters, and whether their relevance is constant throughout the different markets. The original number of trading countries in the data is large, more than 200, but not all of them trade in all of the markets. Thus, to avoid the presence of isolated node-countries and to guarantee an easy and feasible representation of the results, we focus on a subgroup of 64 countries. Table 8 in appendix A reports the list of such countries. In particular, we have considered the median number of countries with which a country trades (that is 7) and removed all the nations that fall under this value. We end up considering a multidimensional networks with the same number of  $n = 64$  nodes and  $K = 10$  networks.

The observed densities range from 0.10 (Plantains market) to 0.28 (Apples market), with a mean of 0.20. Also, the associations<sup>1</sup> between couples of adjacency matrices are really high, ranging in between 0.8 and 0.9, suggesting that countries tend to import/export fruits from a relatively constant set of partners. The observed out-degrees and in-degrees present strong association, as it can be seen in figure 3; thus, the data are a good candidate to test the proposed models.

The heuristic procedure (Section 5.1) suggested the  $VC$  model. Indeed, the average Spearman correlation (Figure 3) computed among couples of observed out-degree distribution, 0.73, is lower than the one computed among couples of observed in-degree distributions, 0.80. However, we fit all the nine models proposed to the data and compute different model selection criteria, to further validate the model proposed by the heuristic procedure. The hyper parameters are fixed as in the simulation setting (Section 5), and  $p = 2$  is the dimension of the latent space, both for plotting reasons and to compare the estimated with the geographical coordinates. AIC (Akaike, 1974), BIC (Schwarz, 1978) and PWAIC1 (Gelman et al., 2014) agreed with the heuristic procedure in the selection of the  $VC$  model. DIC instead opted for the  $VV$  model, the most complex one. Almost all of the selection criteria used and the heuristic procedure agree in proposing the  $VC$  model. Therefore, here we present the results of such model for the FAO fruit trade multidimensional network.

---

<sup>1</sup> The association between any two adjacency matrices,  $k, l = 1, \dots, K$ , is computed comparing the total number of concordant cells between the two matrices and the total number of cells:

$$As(\mathbf{Y}^{(k)}, \mathbf{Y}^{(l)}) = \frac{\sum_{i,j} \mathbf{I}(y_{ij}^{(k)} = y_{ij}^{(l)})}{\sum_{i,j} \mathbf{I}(y_{ij}^{(k)} = y_{ij}^{(l)}) + \sum_{i,j} \mathbf{I}(y_{ij}^{(k)} \neq y_{ij}^{(l)})}.$$

Table 5 reports the top three exporter countries, by means of the estimated sender effects in the different networks. The top exporters are to be interpreted as those countries that tend to export fruit to a large group of trading partners, conditionally on their latent distances from the others. Countries appearing as top exporters in any of the considered fruit markets never show up in the bottom three positions. Also, some countries tend to be top exporters in more than one market. For example, Netherlands (NLD) appears seven times in one of the top three positions. Indeed, Netherlands is amongst the world’s biggest (re-)exporting countries in many fruits and vegetables (FreshPlaza, 2015b). Also, together with Belgium, it is one of the major trade hubs for fresh fruits, importing goods from developing countries and then reselling them (mostly) to the European market (CBI, 2015). Spain (ESP) is estimated to be among the top three exporters in six markets, and first exporter in three of them. Contrary to Netherlands, Spain directly grows most of the fruits it produces. For example, Canary Islands are great pineapples producers. Also, Spain in 2017 became the world’s largest watermelon exporter (FreshPlaza, 2018). Another Mediterranean country is often estimated to be among the top three exporters, as Italy appears five times in a top three. Something similar happens with the estimated bottom three positions; some countries are estimated to be bottom exporters in more than one market. Maldives (MDV) and Kazakhstan (KAZ) appear in the bottom three positions 7 and 6 times, respectively. Indeed, both countries depend largely on imports for most fruit requirements (aquastat, 2011)(Food and Drink, 2017). As for the receiver effects, see Table 6, that are constant across the networks, Germany (DEU) and Netherlands (NLD) are estimated to be first and second overall importers. Indeed, in 2014, the German market accounted for a third of the Dutch (re-)export of fresh fruit (CBI, 2015) (FreshPlaza, 2015a). Also, Germany is estimated to be in the top three exporters ranking for three markets, always jointly with Netherlands. The results are coherent with what observed in the data. For example, in 2013, Germany is the country that imports from an higher number of trading partners, while Maldives never exports. Also, Netherlands is the country that mostly exports to an higher number of trading partners.

The strong similarity in the sender/receiver behaviour of Germany and Netherlands is reflected in the estimates of their latent coordinates, in Figure 4. The coordinates of the two countries almost overlap and are quite close to that of Belgium, another big European (re-)exporter. The estimated latent coordinates do not resemble much the geographical ones; indeed, the Procrustes correlation between the two sets is not high (0.45). The estimated latent space, Figure 4, is characterized by a large number of Asiatic countries placed in the top-left of the space and the majority of the European countries in the bottom-right part. United States are placed in between Asiatic and Oceanic countries. Most of these countries are leading import suppliers of fruits to the United States, thanks to established or pending free trade agreements (Johnson, 2016). The latent space is estimated to be always relevant in the determination of the edge probabilities, and to have similar effect on the different networks. Indeed, Table 7 shows that the estimated scale coefficients  $\beta^{(k)}$  range in (1, 1.60). The same table displays the estimates of the intercepts in the different networks. All of the intercepts correspond to high edge probability values, from 0.971 in the first network, lowest one, to 0.996 in the eight network, highest one. Figure 6 represents the estimated probabilities in the fruit networks, given some values of the distances and of the  $\phi_{ij}^{(k)}$  coefficients. In particular, the probabilities are computed for the first (0.53), second (1.36) and third (2.71) quartiles of the distances. Also, the probabilities are computed for  $\phi_{ij}^{(k)} = (1, 0.5, 0, -0.5)$ . The plot in Figure 6 shows that, even though the latent space is constant, to the same estimated distance corresponds quite

different values of the edge probability, depending on the joint sender/receiver effect and on the network-specific parameters,  $\alpha^{(k)}$  and  $\beta^{(k)}$ .

Last, for illustrative purposes, we display the estimated sender/receiver effects of the countries for the Apples and Pineapples networks (Figure 5). As the receiver effects are constant (y-axis), the plot helps to visualize the different role of each country in the two markets. Two red lines divide the figure in four quadrants. The first and third quadrants contain countries whose estimated sender and receiver effects have same sign. The second (fourth) quadrant displays those countries that have negative (positive) sender effects and positive (negative) receiver effects. Nineteen countries change quadrant in the two markets (Apples and Pineapples). For example, Greece (GRC) and New Zeland (NZL) have both quite an high sender effect in the apple market, but this effect turns negative when trading Pineapples. In general, for the majority of the countries, the estimates of the sender effects tend to be lower in the Pineapples market. Malaysia (MYS) and India (IND) are the only two countries displaying the opposite behaviour; their estimated sender effects are higher in the Pineapples market. Indeed, in 2018, the two countries where both ranked among the world top 20 Pineapples producers ([worldatlas, 2018](#)). Nonetheless, none of the two is estimated to be among the top three Pineapples sending countries in Table 5. However, recall that the sender/receiver estimates are to be interpreted conditionally on the latent distances and that India and Malaysia are located near the majority of the Asiatic countries in the latent space, the top-left panel of Figure 4. Looking at the original data, both the countries, especially Malaysia, tend to export mainly to other Asiatic countries, to which they are close in the latent space. That is, an high probability of trading with Asiatic countries is already guaranteed by the closeness in the latent space. Then, the “residual” contribution given by the sender effect to edge probability does not need to be really high. Instead, Thailand tends to trade with a larger and more variable group of other countries and, therefore, its estimated sender effect in the Pineapples market is higher than those of Malaysia and India.

		$k = 1$	$k = 2$	$k = 3$	$k = 4$	$k = 5$	$k = 6$	$k = 7$	$k = 8$	$k = 9$	$k = 10$
Top	1°	ITA	ESP	ITA	ZAF	ESP	NLD	THA	ESP	DEU	ZAF
	2°	ESP	NLD	FRA	ESP	ITA	THA	NLD	NLD	NLD	NLD
	3°	ZAF	ITA	NZL	EGY	NLD	DEU	DEU	ITA	IND	ESP
Bottom	62°	KWT	QAT	KAZ	RUS	NOR	MDV	LBN	QAT	MAR	QAT
	63°	RUS	MDV	MAR	KAZ	KAZ	KAZ	MDA	NOR	NOR	MDV
	64°	KAZ	HKG	MDV	MDV	MDV	MKD	KAZ	MDV	UKR	MKD

Table 5: Top and bottom three exporters countries, by means of their estimated sender effects.

1°	2°	3°	4°	5°	6°	...	59°	60°	61°	62°	63°	64°
DEU	NLD	BHR	SGP	DNK	POL	...	AUS	EGY	MAR	ZAF	PAK	IRN

Table 6: Top and bottom six importers countries, by means of their estimated receiver effects.



Figure 3: Pairplots of the observed out-degrees and in-degrees of the networks in the fruit multiplex. The upper diagonal matrix represents the associations between the observed out-degrees in any couple of networks, while the lower diagonal shows the association between the in-degrees. The values of the Spearman correlation indexes are reported in the plots.

		$k = 1$	$k = 2$	$k = 3$	$k = 4$	$k = 5$	$k = 6$	$k = 7$	$k = 8$	$k = 9$	$k = 10$
$\alpha$	mean	3.50	5.10	5.46	5.45	5.29	4.91	5.13	5.50	5.07	5.37
	sd	-	0.21	0.22	0.22	0.22	0.20	0.21	0.25	0.23	0.23
$\beta$	mean	1.00	1.34	1.03	1.18	1.13	1.51	1.17	1.36	1.60	1.31
	sd	-	0.06	0.04	0.06	0.05	0.06	0.05	0.06	0.08	0.06

Table 7: Averages and standard deviations of the estimated posterior distributions for the intercept and the scale coefficient parameters in the fruit networks.

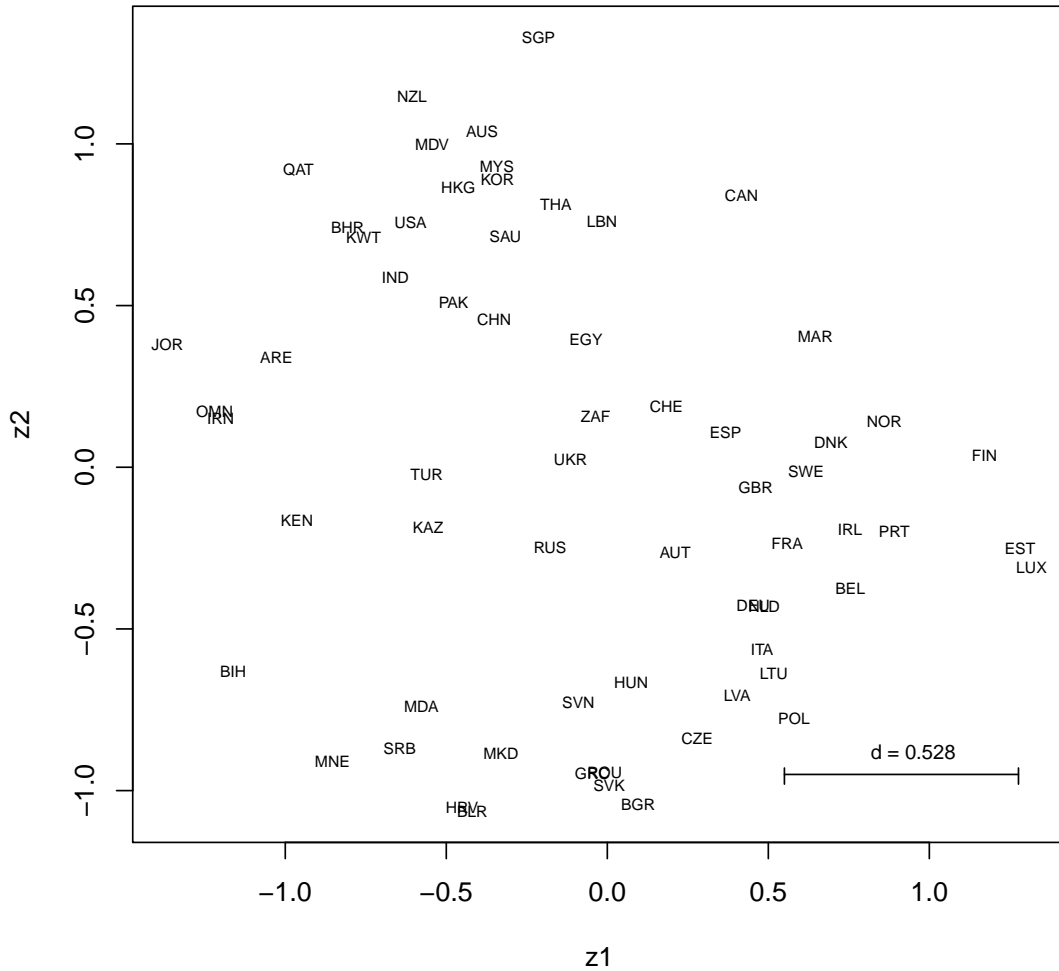


Figure 4: Estimated latent coordinates of the countries in the fruit multiplex. The segments represented in the bottom of the plot displays the value for the first quartile of the estimated distribution of the distances.



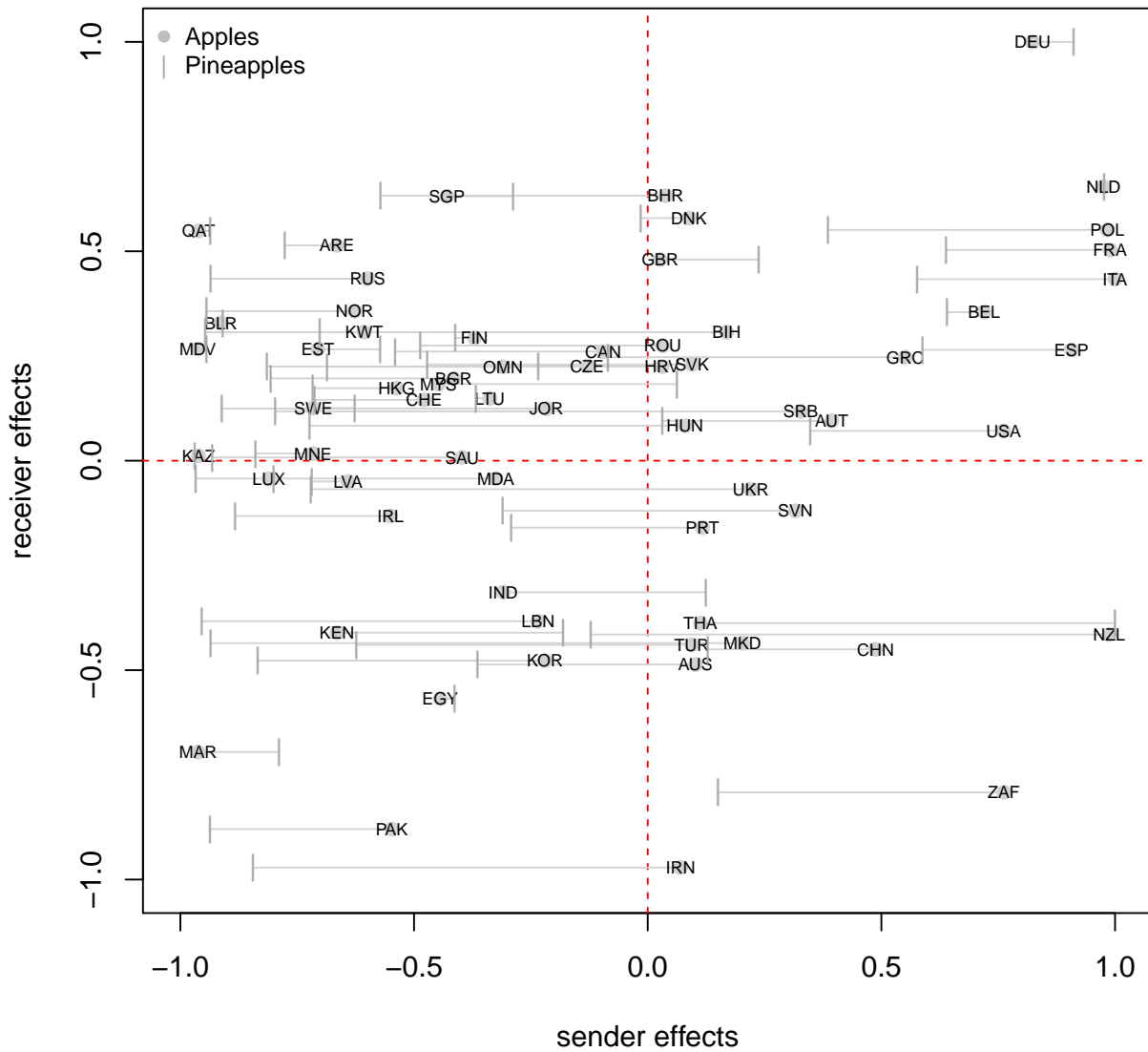


Figure 5: Estimated sender and receiver effects of the countries in the Apples (black) and Pineapples (grey) networks.

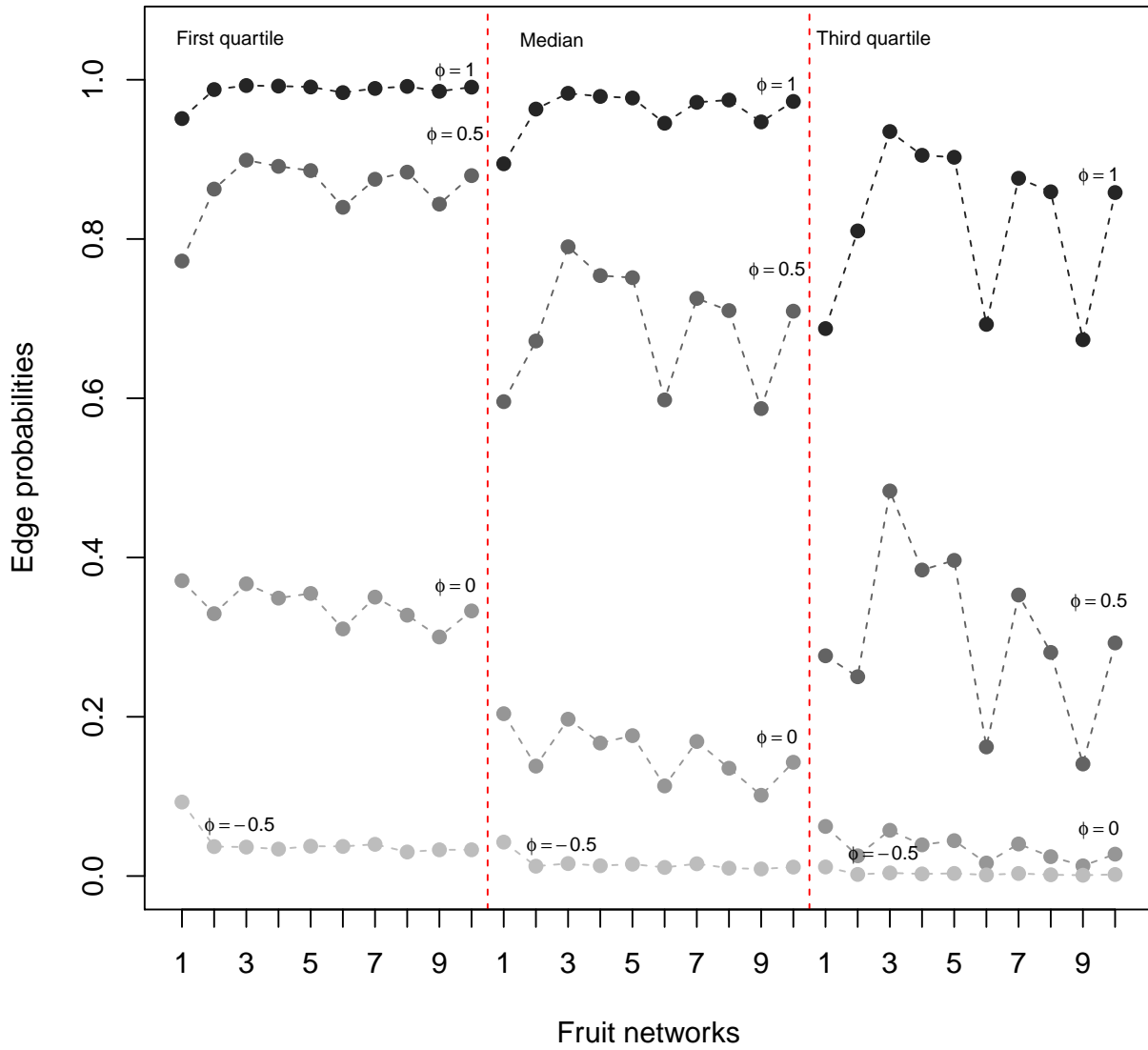


Figure 6: Estimated probabilities in the fruit networks, given different values of the estimated distances ( first quartile, median and third quartile) and different values of the  $\phi_{ij}^{(k)}$  coefficients.

## 7 Discussion

In the present work we have introduced a novel class of Euclidean distance latent space models for multidimensional network data. The models allow to represent transitivity in a parsimonious way, via a single latent space. Also, different levels of nodes degree heterogeneity can be specified. In the spirit of model parsimony, we assume that the type of sender/receiver effect (“Null”, “Constant” and “Variable”) is constant across the views. An interesting relaxation of such hypothesis would be to have the type of effect varying with the networks. Indeed, for example, it may be that a subset  $K^*$  of the  $K$  views has no sender effect, but the remaining networks have constant sender effect. Finding such sub-groups of networks would then become a clustering problem, with extra complexity brought by the allocation of each network to its specific effect-sub-group and the estimation of the number of clusters, which, however, would be bounded in (1, 3).

Also, we have proposed an heuristic procedure for model selection, that allows to choose an appropriate model for observed multiplex data. The procedure permits to bypass a classical model selection step, where all the models would need to be estimated and then compared via some model selection criteria. A preventive selection of the model may be convenient in many real data applications, as model estimation for network data can be quite (computationally) demanding.

An illustrative application on FAO data regarding different fruit trades has been presented, where our method was able to uncover trade patterns and shared similarities among different fruit markets. The data may be an interesting research problem per se, and an interesting extension of the proposed class of models could take in consideration weighted multiplexes, analysing import/export values or quantities. However, considering such weighted edges is non trivial, as the distributions of the exchanged quantities are both right skewed and zero-inflated.

The proposed models will be incorporated shortly in the R package *spaceNet*, already available on *CRAN*.

## References

- Akaike, H. (1974), ‘A New Look at the Statistical Model Identification’, *IEEE Transactions on Automatic Control* **19**(6), 716–723.
- aquastat (2011), ‘Maldives’. [http://www.fao.org/nr/water/aquastat/countries\\_regions/MDV/MDV-CP\\_eng.pdf](http://www.fao.org/nr/water/aquastat/countries_regions/MDV/MDV-CP_eng.pdf).
- CBI (2015), ‘Fresh fruit and vegetables in europe’. [https://www.cbi.eu/sites/default/files/market\\_information/researches/trade-statistics-europe-fresh-fruit-vegetables-2015.pdf](https://www.cbi.eu/sites/default/files/market_information/researches/trade-statistics-europe-fresh-fruit-vegetables-2015.pdf).
- D’Angelo, S., Murphy, T. B. and Alfò, M. (2018), ‘Latent Space Modeling of Multidimensional Networks with Application to the Exchange of Votes in Eurovision Song Contest’, *arXiv* **arXiv:1803.07166** [stat.AP].
- Durante, D. and Dunson, D. (2016), ‘Locally Adaptive Dynamic Networks’, *Annals of Applied Statistics* **10**, 2203–2232.
- FAOStat (2013), ‘Food and agriculture data’. <http://www.fao.org/faostat/en/#home>.
- Food, I. and Drink (2017), ‘Fruit and vegetables in kazakhstan: a billion dollar sector’. <https://www.food-exhibitions.com/Market-Insights/Turkey-and-Eurasia/Fruit-vegetables-in-Kazakhstan>.

- FreshPlaza (2015a), ‘Germany: worldwide 2nd market fresh fruit and vegetables’. <http://www.freshplaza.com/article/138874/Germany-worldwide-2nd-market-fresh-fruit-and-vegetables>.
- FreshPlaza (2015b), ‘Netherlands world’s biggest (re-)exporter for 11 fruit and veg products’. [http://www.freshplaza.com/article/135083/Netherlands-worlds-biggest-\(re-\)exporter-for-11-fruit-and-veg-products](http://www.freshplaza.com/article/135083/Netherlands-worlds-biggest-(re-)exporter-for-11-fruit-and-veg-products).
- FreshPlaza (2018), ‘Spain became the world’s largest watermelon exporter in 2017’. <http://www.freshplaza.com/article/196648/Spain-became-the-worlds-largest-watermelon-exporter-in-2017>.
- Gelman, A., Carlin, J. B., Stern, H. S., Dunson, D. B., Vehtari, A. and Rubin, D. B. (2014), *Bayesian Data Analysis*, CRC press.
- Gollini, I. and Murphy, T. B. (2016), ‘Joint Modeling of Multiple Network Views’, *Journal of Computational and Graphical Statistics* **25**(1), 246–265.
- Hoff, P. (2005), ‘Bilinear mixed-effects models for dyadic data’, *Journal of the American Statistical Association* **100**(469), 286–295.
- Hoff, P. (2011), ‘Hierarchical multilinear models for multiway data’, *Computational Statistics and Data Analysis* **55**, 530–543.
- Hoff, P. D. (2003), ‘Random effects models for network data’, *Breiger, R., Carley, K., Pattinson, P. (Eds.), Dynamic social network modeling and analysis* **126**, 302–322.
- Hoff, P. D., Raftery, A. E. and Handcock, M. S. (2002), ‘Latent Space Approaches to Social Network Analysis’, *Journal of the American Statistical Association* **97**(460), 1090–1098.
- Holland, P. W. and Leinhardt, S. (1981), ‘An exponential family of probability distributions for directed graphs’, *Journal of the American Statistical Association* **76**(373), 33–50.
- Johnson, R. (2016), ‘The u.s. trade situation for fruit and vegetable products’. <https://fas.org/sgp/crs/misc/RL34468.pdf>.
- Krivitsky, P. N., Handcock, M. S., Raftery, A. E. and Hoff, P. D. (2009), ‘Representing degree distributions, clustering, and homophily in social networks with latent cluster random effects models’, *Social Networks* **31**(3), 204–213.
- Salter-Townshend, M. and McCormick, T. H. (2017), ‘Latent Space Models for Multiview Network Data’, *Annals of Applied Statistics* **11**(3), 1217–1244.
- Schwarz, G. (1978), ‘Estimating the Dimension of a Model’, *Annals of Applied Statistics* **6**(2), 461–464.
- Schweinberger, M. and Snijders, T. (2003), ‘Settings in Social Networks: A Measurement Model’, *Sociological Methodology* **33**, 307–341.
- Sewell, D. K. and Chen, Y. (2015), ‘Latent Space Models for Dynamic Networks’, *Journal of the American Statistical Association* **110**(512), 1646–1657.

- Sewell, D. K. and Chen, Y. (2016), ‘Latent space models for dynamic networks with weighted edges’, *Social Networks* **44**, 105–116.
- van Duijn, M., Snijders, T. and Zijlstra, B. (2004), ‘ $p_2$ : a random effects model with covariates for directed graphs’, *Statistica Neerlandica* **58**, 234–254.
- worldatlas (2018), ‘Top pineapple producing countries’. <https://www.worldatlas.com/articles/top-pineapple-producing-countries.html>.

## A Country ISO3 codes

Country name	iso3 code	Country name	iso3 code
Australia	AUS	Malaysia	MYS
Austria	AUT	Maldives	MDV
Bahrain	BHR	Montenegro	MNE
Belarus	BLR	Morocco	MAR
Belgium	BEL	Netherlands	NLD
Bosnia and Herzegovina	BIH	New Zealand	NZL
Bulgaria	BGR	Norway	NOR
Canada	CAN	Oman	OMN
Hong Kong	HKG	Pakistan	PAK
China	CHN	Poland	POL
Croatia	HRV	Portugal	PRT
Czech Republic	CZE	Qatar	QAT
Denmark	DNK	Republic of Korea	KOR
Egypt	EGY	Republic of Moldova	MDA
Estonia	EST	Romania	ROU
Finland	FIN	Russian Federation	RUS
France	FRA	Saudi Arabia	SAU
Germany	DEU	Serbia	SRB
Greece	GRC	Singapore	SGP
Hungary	HUN	Slovakia	SVK
India	IND	Slovenia	SVN
Iran	IRN	South Africa	ZAF
Ireland	IRL	Spain	ESP
Italy	ITA	Sweden	SWE
Jordan	JOR	Switzerland	CHE
Kazakhstan	KAZ	Thailand	THA
Kenya	KEN	Republic of Macedonia	MKD
Kuwait	KWT	Turkey	TUR
Latvia	LVA	Ukraine	UKR
Lebanon	LBN	United Arab Emirates	ARE
Lithuania	LTU	United Kingdom	GBR
Luxembourg	LUX	United States of America	USA

Table 8

## B Estimation: proposal and full conditional distributions

The log-posterior distribution for the eight models with sender and/or receiver effect, presented in section 2, is proportional to:

$$\begin{aligned}
\log\left(P(\alpha, \beta, \theta, \gamma, \mathbf{z}, \mu_\alpha, \mu_\beta, \sigma_\alpha^2, \sigma_\beta^2 | \mathbf{Y})\right) \propto & \\
& \sum_{k=1}^K \sum_{i=1}^n \sum_{j \neq i} h_{ij}^{(k)} \left[ y_{ij}^{(k)} (\alpha^{(k)} \phi_{ij}^{(k)} - \beta^{(k)} d_{ij} - \sum_{f=1}^F \lambda_f x_{ijf}) - \log\left(1 + \exp\{\alpha^{(k)} \phi_{ij}^{(k)} - \beta^{(k)} d_{ij} - \sum_{f=1}^F \lambda_f x_{ijf}\}\right) \right] \\
& - \frac{1}{2} \left\{ \sum_{i=1}^n z_i^2 + \frac{\sum_{k=1}^K (\alpha^{(k)} - \mu_\alpha)^2}{\sigma_\alpha^2} + \frac{\sum_{k=1}^K (\beta^{(k)} - \mu_\beta)^2}{\sigma_\beta^2} + K \log(\sigma_\alpha^2) + K \log(\sigma_\beta^2) + \log(\tau_\alpha \sigma_\alpha^2) + \log(\tau_\beta \sigma_\beta^2) \right\} \\
& + \frac{\mu_\alpha^2}{\tau_\alpha \sigma_\alpha^2} + \frac{\mu_\beta^2}{\tau_\beta \sigma_\beta^2} + \frac{1}{\sigma_\alpha^2} + \frac{1}{\sigma_\beta^2} + \sum_{f=1}^F \left( \frac{(\lambda_f - \mu_{\lambda_f})^2}{\sigma_{\lambda_f}^2} + \log(\sigma_{\lambda_f}^2) + \log(\tau_\lambda \sigma_{\lambda_f}^2) + \frac{(\mu_{\lambda_f} - \mu_\lambda)^2}{\tau_\lambda \sigma_{\lambda_f}^2} + \frac{1}{\sigma_{\lambda_f}^2} \right) \\
& + \left( -\frac{\nu_\alpha}{2} - 1 \right) \log(\sigma_\alpha^2) + \left( -\frac{\nu_\beta}{2} - 1 \right) \log(\sigma_\beta^2) + \sum_{f=1}^F \left( -\frac{\nu_{\lambda_f}}{2} - 1 \right) \log(\sigma_{\lambda_f}^2)
\end{aligned} \tag{8}$$

where, without any loss of information, the latent coordinates are assumed to be univariate.

### B.1 Nuisance parameters

The variances of the intercept and coefficient parameters have Inverse Gamma full conditional distributions

$$\sigma_\alpha^2 | \alpha, \mu_\alpha, \tau_\alpha, \nu_\alpha, K \sim \text{Inv}\Gamma(r_\alpha, R_\alpha); \quad \sigma_\beta^2 | \beta, \mu_\beta, \tau_\beta, \nu_\beta, K \sim \text{Inv}\Gamma(r_\beta, R_\beta),$$

with parameters:

$$r_x = \frac{\nu_x + K + 1}{2}, \quad R_x = \frac{\tau_x + \tau_x \sum_{k=1}^K (x^{(k)} - \mu_x)^2 + \mu_x^2}{2\tau_x}.$$

The nuisance parameters  $\mu_\alpha, \mu_\beta$  are distributed as truncated normal distributions:

$$\begin{aligned}
\mu_\alpha | \alpha, \sigma_\alpha^2, \tau_\alpha, m_\alpha, K &\sim N_{[0, \infty]} \left( \frac{\tau_\alpha \sum_{k=1}^K \alpha^{(k)} + m_\alpha}{1 + K\tau_\alpha}, \frac{\tau_\alpha \sigma_\alpha^2}{1 + K\tau_\alpha} \right), \\
\mu_\beta | \beta, \sigma_\beta^2, \tau_\beta, m_\beta, K &\sim N_{[0, \infty]} \left( \frac{\tau_\beta \sum_{k=1}^K \beta^{(k)} + m_\beta}{1 + K\tau_\beta}, \frac{\tau_\beta \sigma_\beta^2}{1 + K\tau_\beta} \right).
\end{aligned}$$

### B.2 Latent positions

The proposal distribution for the  $i^{\text{th}}$  latent coordinate is derived from the log-posterior distribution of the model in equation 8. The logarithmic term in the log-likelihood, which is indeed a LSE function, is approximated with its lower bound.

$$\tilde{z}_i | \mathbf{Y}, \alpha, \theta_i, \gamma, \beta, \lambda, \mathbf{x}_i, \mathbf{D}, K \sim N(\mu_{\tilde{z}_i}, \sigma_{\tilde{z}_i}^2),$$

where

$$\mu_{\tilde{z}_i} = \sigma_{\tilde{z}_i}^2 \left( 2 \sum_{k=1}^K \beta^{(k)} \sum_{j \neq i} h_{ij}^{(k)} (y_{ij}^{(k)} - w_{ij}^{(k)}) z_j \right), \quad \sigma_{\tilde{z}_i}^2 = \left( 1 + 2 \sum_{k=1}^K \beta^{(k)} \sum_{j \neq i} h_{ij}^{(k)} |y_{ij}^{(k)} - w_{ij}^{(k)}| \right)^{-1}.$$

where  $w_{ij}^{(k)}$  is a binary indicator variable, defined as:

$$w_{ij}^{(k)} = \begin{cases} 1 & \text{if } \alpha^{(k)}\phi_{ij}^{(k)} - \beta^{(k)}d_{ij} - \sum_{f=1}^F \lambda_f x_{ijf} > 0 \\ 0 & \text{if } \alpha^{(k)}\phi_{ij}^{(k)} - \beta^{(k)}d_{ij} - \sum_{f=1}^F \lambda_f x_{ijf} \leq 0 \end{cases},$$

### B.3 Intercept parameters

The proposal distribution for the  $k^{\text{th}}$  intercept parameter  $\alpha^{(k)}$  is derived from the log-posterior distribution, where the logarithmic term is approximated via its second order Taylor expansion in  $\alpha^{(k)} = \mu_\alpha$ . Defining  $E^{(k)} = \sum_{i=1}^n \sum_{j \neq i} h_{ij}^{(k)} y_{ij}^{(k)} \phi_{ij}^{(k)}$ , the proposal distribution for intercept  $\alpha^{(k)}$  is taken to be:

$$\tilde{\alpha}^{(k)} \mid \mathbf{Y}, \mathbf{D}, \mathbf{H}, \beta^{(k)}, \theta^{(k)}, \gamma^{(k)}, \lambda, \mathbf{X}, \mu_\alpha, \sigma_\alpha^2 \sim N\left(\mu_{\tilde{\alpha}^{(k)}}, \sigma_{\tilde{\alpha}^{(k)}}^2\right),$$

with

$$\begin{aligned} \mu_{\tilde{\alpha}^{(k)}} &= \sigma_{\tilde{\alpha}^{(k)}}^2 \left\{ E^{(k)} - \sum_{i=1}^n \sum_{j \neq i} \frac{h_{ij}^{(k)} \phi_{ij}^{(k)} \exp\{\mu_\alpha \phi_{ij}^{(k)} - \beta^{(k)} d_{ij} - \sum_{f=1}^F \lambda_f x_{ijf}\}}{1 + \exp\{\mu_\alpha \phi_{ij}^{(k)} - \beta^{(k)} d_{ij} - \sum_{f=1}^F \lambda_f x_{ijf}\}} \right\} + \mu_\alpha, \\ \sigma_{\tilde{\alpha}^{(k)}}^2 &= \left\{ \sum_{i=1}^n \sum_{j \neq i} \frac{h_{ij}^{(k)} (\phi_{ij}^{(k)})^2 \exp\{\mu_\alpha \phi_{ij}^{(k)} - \beta^{(k)} d_{ij} - \sum_{f=1}^F \lambda_f x_{ijf}\}}{(1 + \exp\{\mu_\alpha \phi_{ij}^{(k)} - \beta^{(k)} d_{ij} - \sum_{f=1}^F \lambda_f x_{ijf}\})^2} + \frac{1}{\sigma_\alpha^2} \right\}^{-1} \end{aligned}$$

### B.4 Coefficient parameters (distances)

The proposal distribution for the  $k^{\text{th}}$  coefficient parameter  $\beta^{(k)}$  is derived from the log-posterior distribution, where the logarithmic term is approximated via its second order Taylor expansion in  $\beta^{(k)} = \mu_\beta$ .

Then, the proposal distribution specified for intercept coefficient  $k$  is:

$$\tilde{\beta}^{(k)} \mid \mathbf{Y}, \mathbf{D}, \mathbf{H}, \alpha^{(k)}, \theta^{(k)}, \gamma^{(k)}, \lambda, \mathbf{X}, \mu_\beta, \sigma_\beta^2 \sim N\left(\mu_{\tilde{\beta}^{(k)}}, \sigma_{\tilde{\beta}^{(k)}}^2, n\right),$$

where

$$\begin{aligned} \mu_{\tilde{\beta}^{(k)}} &= \sigma_{\tilde{\beta}^{(k)}}^2 \left\{ \sum_{i=1}^n \sum_{j \neq i} h_{ij}^{(k)} d_{ij} \left( \frac{\exp\{\alpha^{(k)} \phi_{ij}^{(k)} - \mu_\beta d_{ij} - \sum_{f=1}^F \lambda_f x_{ijf}\}}{1 + \exp\{\alpha^{(k)} \phi_{ij}^{(k)} - \mu_\beta d_{ij} - \sum_{f=1}^F \lambda_f x_{ijf}\}} - y_{ij}^{(k)} \right) \right\} + \mu_\beta, \\ \sigma_{\tilde{\beta}^{(k)}}^2 &= \left\{ \sum_{i=1}^n \sum_{j \neq i} \frac{h_{ij}^{(k)} d_{ij}^2 \exp\{\alpha^{(k)} \phi_{ij}^{(k)} - \mu_\beta d_{ij} - \sum_{f=1}^F \lambda_f x_{ijf}\}}{(1 + \exp\{\alpha^{(k)} \phi_{ij}^{(k)} - \mu_\beta d_{ij} - \sum_{f=1}^F \lambda_f x_{ijf}\})^2} + \frac{1}{\sigma_\beta^2} \right\}^{-1} \end{aligned}$$

### B.5 Coefficient parameters (covariates)

The proposal distribution for  $\lambda_f$  is:

$$\tilde{\lambda}_f \mid \alpha, \beta, \lambda, \gamma, \theta, \mu_{\lambda_f}, \sigma_{\lambda_f}^2, \mathbf{D}, \mathbf{H}, \mathbf{X}, \mathbf{Y} \sim N_{(0, \infty)}\left(\mu_{\tilde{\lambda}_f}, \sigma_{\tilde{\lambda}_f}^2\right),$$

where

$$\begin{aligned} \mu_{\tilde{\lambda}_f} &= \sigma_{\tilde{\lambda}_f}^2 \left[ \sum_{k=1}^K \left( \sum_{i=1}^n \sum_{j \neq i} \frac{x_{ijf} h_{ij}^{(k)} \exp(\alpha^{(k)} \phi_{ij}^{(k)} - \beta^{(k)} d_{ij} - \sum_{l \neq f} \lambda_l x_{ijl})}{1 + \exp(\alpha^{(k)} \phi_{ij}^{(k)} - \beta^{(k)} d_{ij} - \sum_{l \neq f} \lambda_l x_{ijl})} - y_{ij}^{(k)} x_{ijf} \right) \right] + \mu_{\lambda_f}, \\ \sigma_{\tilde{\lambda}_f}^2 &= \left\{ \sum_{k=1}^K \sum_{i=1}^n \sum_{j \neq i} \frac{h_{ij}^{(k)} x_{ijf}^2 \exp(\alpha^{(k)} \phi_{ij}^{(k)} - \beta^{(k)} d_{ij} - \sum_{l \neq f} \lambda_l x_{ijl})}{(1 + \exp(\alpha^{(k)} \phi_{ij}^{(k)} - \beta^{(k)} d_{ij} - \sum_{l \neq f} \lambda_l x_{ijl}))^2} + \frac{1}{\sigma_{\lambda_f}^2} \right\}^{-1}. \end{aligned}$$



## B.6 Sender and receiver parameters

To define proposal distributions for the sender and receiver parameter, we consider only the relevant part of the posterior distribution. In particular, we will derive them from the log-likelihood of the model, that is, the first line of the log-posterior distribution presented in equation 8,

$$\sum_{k=1}^K \sum_{i=1}^n \sum_{j \neq i} h_{ij}^{(k)} \left[ y_{ij}^{(k)} (\alpha^{(k)} \phi_{ij}^{(k)} - \beta^{(k)} d_{ij} - \sum_{f=1}^F \lambda_f x_{ijf}) - \log \left( 1 + \exp \left\{ \alpha^{(k)} \phi_{ij}^{(k)} - \beta^{(k)} d_{ij} - \sum_{f=1}^F \lambda_f x_{ijf} \right\} \right) \right].$$

### B.6.1 Sender parameters

When the sender effect is variable across the networks, we need to propose a new value for the  $i^{(th)}$  sender parameter in the  $k^{th}$  network at the  $t^{th}$  iteration of the MCMC algorithm. We start by approximating the logarithmic term in the log-likelihood via its second order Taylor's expansion in  $\theta_i^{(k)t} \approx \theta_i^{(k)t-1}$ :

$$\begin{aligned} \log \left( 1 + \exp \left\{ \alpha^{(k)} \phi_{ij}^{(k)t} - \beta^{(k)} d_{ij} \right\} \right) &= \log \left( 1 + \exp \left\{ \frac{\alpha^{(k)} \theta_i^{(k)t}}{g} + \frac{\alpha^{(k)} \gamma_j^{(k)}}{g} - \beta^{(k)} d_{ij} \right\} \right) \\ &\approx \left( \theta_i^{(k)t} - \theta_i^{(k)t-1} \right) \left\{ \frac{\frac{\alpha^{(k)}}{g} \exp \left\{ \frac{\alpha^{(k)} \theta_i^{(k)t-1}}{g} + \frac{\alpha^{(k)} \gamma_j^{(k)}}{g} - \beta^{(k)} d_{ij} \right\}}{1 + \exp \left\{ \frac{\alpha^{(k)} \theta_i^{(k)t-1}}{g} + \frac{\alpha^{(k)} \gamma_j^{(k)}}{g} - \beta^{(k)} d_{ij} \right\}} \right\} \\ &\quad + \frac{1}{2} \left( \theta_i^{(k)t} - \theta_i^{(k)t-1} \right)^2 \left\{ \frac{\left( \frac{\alpha^{(k)}}{g} \right)^2 \exp \left\{ \frac{\alpha^{(k)} \theta_i^{(k)t-1}}{g} + \frac{\alpha^{(k)} \gamma_j^{(k)}}{g} - \beta^{(k)} d_{ij} \right\}}{\left( 1 + \exp \left\{ \frac{\alpha^{(k)} \theta_i^{(k)t-1}}{g} + \frac{\alpha^{(k)} \gamma_j^{(k)}}{g} - \beta^{(k)} d_{ij} \right\} \right)^2} \right\} + const \end{aligned}$$

Then, the logarithmic term is substituted with its approximation. The approximated log-likelihood is now a quadratic function in  $\theta_i^{(k)t}$ , which permits to define the following proposal distribution

$$\tilde{\theta}_i^{(k)t} \mid \alpha^{(k)}, \beta^{(k)}, \lambda, \gamma^{(k)}, \theta_i^{(k)t-1}, \mathbf{D}, \mathbf{H}, \mathbf{X}, \mathbf{Y} \sim N_{(-1,1)} \left( \mu_{\tilde{\theta}_i^{(k)t}}, \sigma_{\tilde{\theta}_i^{(k)t}}^2 \right)$$

where

$$\begin{aligned} \mu_{\tilde{\theta}_i^{(k)t}} &= \left[ \frac{\alpha^{(k)}}{g} \sum_{j \neq i} h_{ij}^{(k)} \left( y_{ij}^{(k)} - \frac{\exp(\alpha^{(k)} \phi_{ij}^{(k)t-1} - \beta^{(k)} d_{ij})}{1 + \exp(\alpha^{(k)} \phi_{ij}^{(k)t-1} - \beta^{(k)} d_{ij})} \right) \right] \sigma_{\tilde{\theta}_i^{(k)t}}^2 + \theta_i^{(k)t-1} \\ \sigma_{\tilde{\theta}_i^{(k)t}}^2 &= \left[ \left( \frac{\alpha^{(k)}}{g} \right)^2 \sum_{j \neq i} h_{ij}^{(k)} \left( \frac{\exp(\alpha^{(k)} \phi_{ij}^{(k)t-1} - \beta^{(k)} d_{ij})}{\left( 1 + \exp(\alpha^{(k)} \phi_{ij}^{(k)t-1} - \beta^{(k)} d_{ij}) \right)^2} \right) \right]^{-1} \end{aligned}$$

Instead, when the sender effect is constant, the logarithmic term in the log-likelihood is approximated with its second order Taylor's expansion in  $\theta_i^t \approx \theta_i^{t-1}$  and the resulting proposal distribution is:

$$\tilde{\theta}_i^t \mid \alpha, \beta, \lambda, \gamma, \theta_i^{t-1}, \mathbf{D}, \mathbf{H}, \mathbf{X}, \mathbf{Y} \sim N_{(-1,1)} \left( \mu_{\tilde{\theta}_i^t}, \sigma_{\tilde{\theta}_i^t}^2 \right)$$

where

$$\begin{aligned} \mu_{\tilde{\theta}_i^t} &= \left[ \sum_{k=1}^K \frac{\alpha^{(k)}}{g} \sum_{j \neq i} h_{ij}^{(k)} \left( y_{ij}^{(k)} - \frac{\exp(\alpha^{(k)} \phi_{ij}^{t-1} - \beta^{(k)} d_{ij})}{1 + \exp(\alpha^{(k)} \phi_{ij}^{t-1} - \beta^{(k)} d_{ij})} \right) \right] \sigma_{\tilde{\theta}_i^t}^2 + \theta_i^{t-1} \\ \sigma_{\tilde{\theta}_i^t}^2 &= \left[ \sum_{k=1}^K \left( \frac{\alpha^{(k)}}{g} \right)^2 \sum_{j \neq i} h_{ij}^{(k)} \left( \frac{\exp(\alpha^{(k)} \phi_{ij}^{t-1} - \beta^{(k)} d_{ij})}{\left( 1 + \exp(\alpha^{(k)} \phi_{ij}^{t-1} - \beta^{(k)} d_{ij}) \right)^2} \right) \right]^{-1} \end{aligned}$$

The proposal distribution defined depend on the previous value of the parameter of interest, as in random walk proposals, but also on the current configuration of all the other parameters. This allows to explore efficiently

the parameter space for the  $\theta_i^{(k)}$ s: Indeed, classical random walks are usually slow in the exploration of the parameter space and, when employed in the estimation procedure of this class of models, they returned unstable chains. ‘‘Correcting’’ the random walk by incorporating the past value of the sender parameter of interest in a more complex parametrization of the proposal distribution has proven to be a valid approach to estimate these parameters.

### B.6.2 Receiver parameters

The proposal distributions for the receiver parameters, both in the variable and in the constant case, are recovered with the same procedure used to define those of the sender parameters. The only, obvious, difference is that the logarithmic term of the log-likelihood is approximated in the receiver parameter. Then, the proposal distributions for the  $j^{\text{th}}$  receiver parameter at the  $t^{\text{th}}$  iteration are:

- If the effect is variable:

$$\tilde{\gamma}_j^{(k)t} \mid \alpha^{(k)}, \beta^{(k)}, \lambda, \theta^{(k)}, \gamma_j^{(k)t-1}, \mathbf{D}, \mathbf{H}, \mathbf{X}, \mathbf{Y} \sim N_{(-1,1)}\left(\mu_{\tilde{\gamma}_j^{(k)t}}, \sigma_{\tilde{\gamma}_j^{(k)t}}^2\right)$$

where

$$\mu_{\tilde{\gamma}_j^{(k)t}} = \left[ \frac{\alpha^{(k)}}{g} \sum_{i \neq j} h_{ij}^{(k)} \left( y_{ij}^{(k)} - \frac{\exp(\alpha^{(k)} \phi_{ij}^{(k)t-1} - \beta^{(k)} d_{ij})}{1 + \exp(\alpha^{(k)} \phi_{ij}^{(k)t-1} - \beta^{(k)} d_{ij})} \right) \right] \sigma_{\tilde{\gamma}_j^{(k)t}}^2 + \gamma_j^{(k)t-1}$$

$$\sigma_{\tilde{\gamma}_j^{(k)t}}^2 = \left[ \left( \frac{\alpha^{(k)}}{g} \right)^2 \sum_{i \neq j} h_{ij}^{(k)} \left( \frac{\exp(\alpha^{(k)} \phi_{ij}^{(k)t-1} - \beta^{(k)} d_{ij})}{\left( 1 + \exp(\alpha^{(k)} \phi_{ij}^{(k)t-1} - \beta^{(k)} d_{ij}) \right)^2} \right) \right]^{-1}.$$

- If the effect is constant:

$$\tilde{\gamma}_j^t \mid \alpha, \beta, \lambda, \theta, \gamma_j^{t-1}, \mathbf{D}, \mathbf{H}, \mathbf{X}, \mathbf{Y} \sim N_{(-1,1)}\left(\mu_{\tilde{\gamma}_j^t}, \sigma_{\tilde{\gamma}_j^t}^2\right)$$

where

$$\mu_{\tilde{\gamma}_j^t} = \left[ \sum_{k=1}^K \frac{\alpha^{(k)}}{g} \sum_{i \neq j} h_{ij}^{(k)} \left( y_{ij}^{(k)} - \frac{\exp(\alpha^{(k)} \phi_{ij}^{(k)t-1} - \beta^{(k)} d_{ij})}{1 + \exp(\alpha^{(k)} \phi_{ij}^{(k)t-1} - \beta^{(k)} d_{ij})} \right) \right] \sigma_{\tilde{\gamma}_j^t}^2 + \gamma_j^{t-1}$$

$$\sigma_{\tilde{\gamma}_j^t}^2 = \left[ \sum_{k=1}^K \left( \frac{\alpha^{(k)}}{g} \right)^2 \sum_{i \neq j} h_{ij}^{(k)} \left( \frac{\exp(\alpha^{(k)} \phi_{ij}^{(k)t-1} - \beta^{(k)} d_{ij})}{\left( 1 + \exp(\alpha^{(k)} \phi_{ij}^{(k)t-1} - \beta^{(k)} d_{ij}) \right)^2} \right) \right]^{-1}.$$

### B.6.3 Undirected networks

The proposal distributions for the  $\delta_i^{(k)}$  parameters, both in the variable and in the constant case, are recovered with the same procedure used to define those of the sender and the receiver parameters. This time, the logarithmic term in the log-likelihood, which this time is defined via the edge probabilities in equation 7, is approximated in the  $i^{\text{th}}$  parameter. The proposal distributions for the  $i^{\text{th}}$  parameter at the  $t^{\text{th}}$  iteration are:

- If the effect is variable:

$$\tilde{\delta}_i^{(k)t} \mid \alpha^{(k)}, \beta^{(k)}, \lambda, \delta_i^{(k)t-1}, \mathbf{D}, \mathbf{H}, \mathbf{X}, \mathbf{Y} \sim N_{(-1,1)}\left(\mu_{\tilde{\delta}_i^{(k)t}}, \sigma_{\tilde{\delta}_i^{(k)t}}^2\right)$$

where

$$\mu_{\tilde{\delta}_i^{(k)t}} = \left[ \frac{\alpha^{(k)}}{g} \sum_{j \neq i} h_{ij}^{(k)} \left( y_{ij}^{(k)} - \frac{\exp(\alpha^{(k)} \phi_{ij}^{(k)t-1} - \beta^{(k)} d_{ij})}{1 + \exp(\alpha^{(k)} \phi_{ij}^{(k)t-1} - \beta^{(k)} d_{ij})} \right) \right] \sigma_{\tilde{\delta}_i^{(k)t}}^2 + \delta_i^{(k)t-1}$$

$$\sigma_{\tilde{\delta}_i^{(k)t}}^2 = \left[ \left( \frac{\alpha^{(k)}}{g} \right)^2 \sum_{j \neq i} h_{ij}^{(k)} \left( \frac{\exp(\alpha^{(k)} \phi_{ij}^{(k)t-1} - \beta^{(k)} d_{ij})}{\left( 1 + \exp(\alpha^{(k)} \phi_{ij}^{(k)t-1} - \beta^{(k)} d_{ij}) \right)^2} \right) \right]^{-1}.$$

- If the effect is constant:

$$\tilde{\delta}_i^t \mid \alpha, \beta, \lambda, \delta^{t-1}, \mathbf{D}, \mathbf{H}, \mathbf{X}, \mathbf{Y} \sim N_{(-1,1)} \left( \mu_{\tilde{\delta}_i^t}, \sigma_{\tilde{\delta}_i^t}^2 \right)$$

where

$$\mu_{\tilde{\delta}_i^t} = \left[ \sum_{k=1}^K \frac{\alpha^{(k)}}{g} \sum_{j \neq i} h_{ij}^{(k)} \left( y_{ij}^{(k)} - \frac{\exp(\alpha^{(k)} \phi_{ij}^{t-1} - \beta^{(k)} d_{ij})}{1 + \exp(\alpha^{(k)} \phi_{ij}^{t-1} - \beta^{(k)} d_{ij})} \right) \right] \sigma_{\tilde{\delta}_i^t}^2 + \delta_i^{t-1}$$

$$\sigma_{\tilde{\delta}_i^t}^2 = \left[ \sum_{k=1}^K \left( \frac{\alpha^{(k)}}{g} \right)^2 \sum_{j \neq i} h_{ij}^{(k)} \left( \frac{\exp(\alpha^{(k)} \phi_{ij}^{t-1} - \beta^{(k)} d_{ij})}{\left( 1 + \exp(\alpha^{(k)} \phi_{ij}^{t-1} - \beta^{(k)} d_{ij}) \right)^2} \right) \right]^{-1}.$$

## C Simulation results

### C.1 Block I

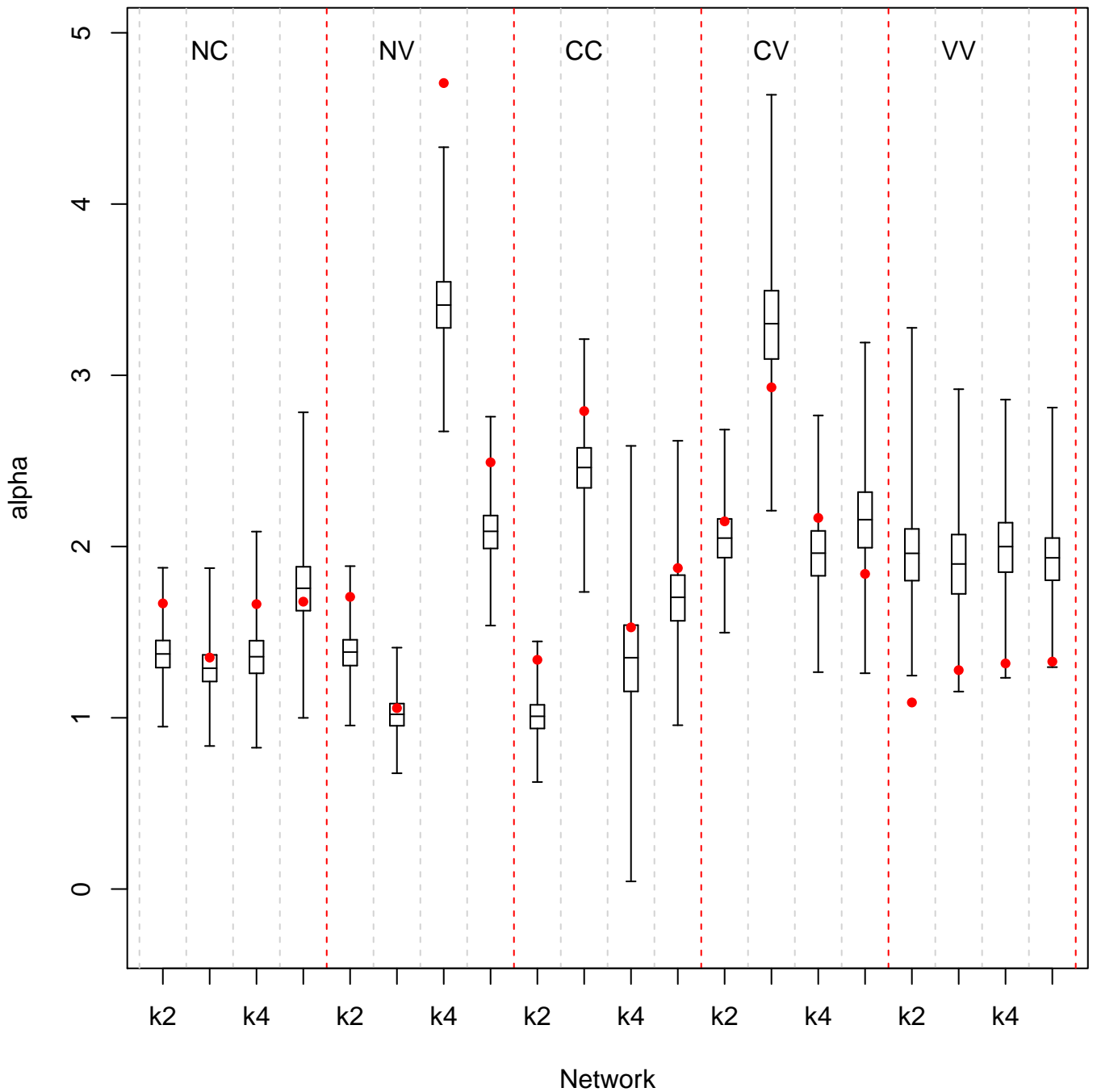


Figure 7: Boxplots of the estimated posterior distributions of the intercept parameters of the multidimensional networks with  $n = 50$  and  $K = 5$  simulated in the block I. Red dots indicate the true, simulated, values of the intercepts .

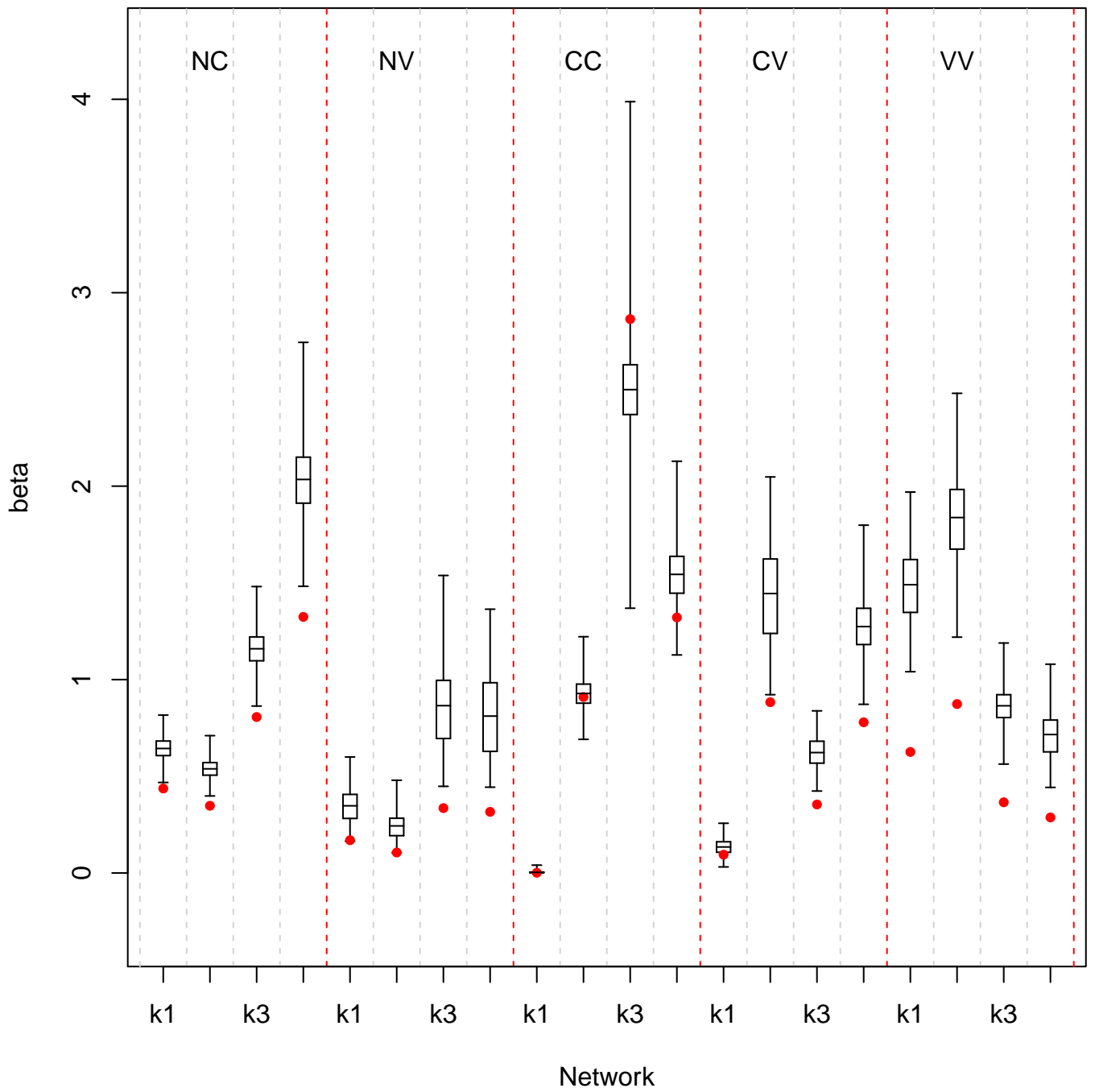


Figure 8: Boxplots of the estimated posterior distributions of the coefficient parameters of the multidimensional networks with  $n = 50$  and  $K = 5$  simulated in the block I. Red dots indicate the true, simulated, values of the coefficients.

## D Heuristic model search

		Simulated								
		NN	CN	NC	CC	VN	NV	VC	CV	VV
Selected (%)	NN	<b>82</b>	0	0	18	0	0	0	0	0
	CN	0	<b>96</b>	0	3	0	0	0	1	0
	NC	0	0	<b>96</b>	3	0	0	1	0	0
	CC	12	0	1	<b>85</b>	0	0	1	1	0
	VN	0	0	0	0	<b>87</b>	0	13	0	0
	NV	0	0	0	0	0	<b>87</b>	0	13	0
	VC	0	0	0	2	8	0	<b>90</b>	0	0
	CV	0	0	0	2	0	9	0	<b>89</b>	0
	VV	0	0	0	19	0	0	0	0	<b>81</b>

Table 9: Percentage of time each type of model was selected versus the true, simulated models. The dimensions of the simulated multidimensional networks are  $n = 50$  and  $K = 10$ .

		Simulated								
		NN	CN	NC	CC	VN	NV	VC	CV	VV
Selected (%)	NN	<b>86</b>	0	0	14	0	0	0	0	0
	CN	0	<b>96</b>	0	4	0	0	0	0	0
	NC	0	0	<b>96</b>	4	0	0	0	0	0
	CC	16	0	0	<b>84</b>	0	0	0	0	1
	VN	0	0	0	0	<b>92</b>	0	8	0	0
	NV	0	0	0	0	0	<b>92</b>	0	8	0
	VC	0	0	0	1	13	0	<b>86</b>	0	0
	CV	0	0	0	1	0	13	0	<b>86</b>	0
	VV	0	0	0	10	0	0	0	0	<b>90</b>

Table 10: Percentage of time each type of model was selected versus the true, simulated models. The dimensions of the simulated multidimensional networks are  $n = 65$  and  $K = 10$ .